Free Radical Research, December 2007; 41(12): 1326–1337

informa
healthcare

Involvement of reactive oxygen species in Microcystin-LR-induced cytogenotoxicity

QINGQING NONG[1], MASAHARU KOMATSU[1], KIMIKO IZUMO[1], HIROKO P. INDO[2], BAOHUI XU[1], KOHJI AOYAMA[1], HIDEYUKI J. MAJIMA[2], MASAHISA HORIUCHI[1], KANEHISA MORIMOTO[3], & TORU TAKEUCHI[1]

[1]*Department of Environmental Medicine,* [2]*Department of Oncology and Department of Space Environmental Medicine, Graduate School of Medical and Dental Sciences, Kagoshima University, 8-35-1 Sakuragaoka, Kagoshima 890–8544, Japan, and* [3]*Department of Social and Environmental Medicine, Osaka University Graduate School of Medicine, 2–2 Yamadaoka, Suita, Osaka 565–0871, Japan*

Accepted by: Professor M. Smith

(Received 17 July 2007; in revised form 19 September 2007)

Abstract
Microcystin-LR (MCLR) is a potent hepatotoxin. Oxidative stress is thought to be implicated in the cytotoxicity of MCLR, but the mechanisms by which MCLR produces reactive oxygen species (ROS) are still unclear. This study investigated the role and possible sources of ROS generation in MCLR-induced cytogenotoxicity in HepG2, a human hepatoma cell line. MCLR increased DNA strand breaks, 8-hydroxydeoxiguanosine formation, lipid peroxidation, as well as LDH release, all of which were inhibited by ROS scavengers. ROS scavengers partly suppressed MCLR-induced cytotoxicity determined by the MTT assay. MCLR induced the generation of ROS, as confirmed by confocal microscopy with 2-[6-(4′-hydroxy)phenoxy-3H-xanthen-3-on-9-yl]benzoic acid, and upregulated the expression of CYP2E1 mRNA. In addition, CYP2E1 inhibitors chlormethiazole and diallyl sulphide inhibited both ROS generation and cytotoxicity induced by MCLR. The results suggest that ROS contribute to MCLR-induced cytogenotoxicity. CYP2E1 might be a potential source responsible for ROS generation by MCLR.

Keywords: *Microcystin-LR, cytogenotoxicity, reactive oxygen species (ROS), oxidative damage, CYP2E1.*

Introduction

Microcystins are potent hepatotoxins, produced by several cyanobacteria including *Microcystis*, *Anabaena* and *Oscillatoria*, that often form blooms in waters where the nutrients are enriched. Exposure to these toxins causes deaths of livestock, allergy, gastrointestinal disorders and liver diseases in humans [1,2]. So far, more than 70 structural analogues of microcystins have been identified [3]. Microcystin-LR (MCLR) is the most commonly encountered microcystin with strong hepatotoxicity and tumour promotion activity [4]. It inhibits eukaryote serine/threonine protein phosphatases (PP) 1 and 2A, leading to increases in protein phosphorylation [5–7].

Recently, it has been reported that organic anion transporting polypeptides (OATP)1B1 and OATP1B3 are required for the hepatic uptake of MCLR [8–10]. MCLR showed potent cytotoxicity in OATP-transfected cells such as cervical adenocarcinoma cells HeLa-OATP, human embryonic kidney cells HEK293-OATP and *xenopus* oocytes-OATP.

Correspondence: Toru Takeuchi, Department of Environmental Medicine, Graduate School of Medical and Dental Sciences, Kagoshima University, 8-35-1 Sakuragaoka, Kagoshima 890–8544, Japan. Tel: 81 99 2755288. Fax: 81 99 2658434. Email: takeuchi@m.kufm.kagoshima-u.ac.jp

ISSN 1071-5762 print/ISSN 1029-2470 online
DOI: 10.1080/10715760701704599

However, these OATP-transfected cells have been reported to be more sensitive to MCLR than primary rat hepatocytes [9,10], implying that there are metabolic differences between transfected non-hepatic cells and primary hepatocytes. In OATP1B1- and OATP1B3-transfected HeLa cells, MCLR induced cytotoxicity mainly through inhibition of PP2A, while reactive oxygen species (ROS) may not be involved [9]. On the other hand, Ding et al. [11] found that exposure to MCLR (1 μM) caused rapid formation of ROS in primary rat hepatocytes. ROS may be major causes of hepatocyte apoptosis induced by MCLR both *in vivo* and *in vitro* [12–17]. These previous findings suggest that MCLR may have different cytotoxic effects in different cell types due to different metabolic system and ROS-generating system.

A human hepatoma cell line, HepG2, retains the activities of various phase I and phase II drug metabolizing enzymes which play crucial roles in the activation/detoxification of xenobiotics, reflecting the metabolism status similar to those of human hepatocytes. In addition, ROS-generating enzymes such as cytochrome P450 and NADPH oxidase can be induced in HepG2 cells [18–21]. Because MCLR is a potent hepatotoxin and the main target organ of MCLR is liver, the use of HepG2 cells with metabolic system similar to original human hepatocytes may properly estimate the hepatotoxic effects of MCLR. Moreover HepG2 cells were reported to internalize MCLR [22] and to respond to MCLR at similar concentrations that induced cytotoxicity in primary rat hepatocytes [23–25]. Several reports have described the induction of oxidative stress by MCLR; however, there is no report regarding the source and mechanisms responsible for the generation of ROS induced by MCLR.

In this study, we investigated the cytogenotoxic effects of MCLR on HepG2 cells, particularly the involvement of oxidative damages including DNA strand breaks, 8-hydroxydeoxiguanosine (8OHdG) formation and lipid peroxidation. Further, we also analysed the mechanisms by which MCLR produces ROS.

Materials and methods

Cells and reagents

HepG2 cells were donated from the Cell Resource Centre for Biomedical Research Institute of Development, Ageing and Cancer, Tohoku University (Sendai, Japan) and grown with Dulbecco's Modified Eagle's Medium (Sigma, St. Louis, MO) containing 10% heat-inactivated foetal calf serum, 100 U/ml penicillin and 100 μg/ml streptomycin.

MCLR was purchased from ALEXIS (Lausen, Switzerland). MCLR was dissolved in dimethyl sulphoxide (DMSO, Sigma) and then diluted in Dulbecco's phosphate-buffered saline (DPBS, Sigma). The final concentration of DMSO in culture medium was 0.1%. Mouse anti-8OHdG monoclonal antibody (mAb, clone IF7, mouse IgG1) and mouse IgG1 isotype control were purchased from R & D Systems (Minneapolis, MN) and Sigma, respectively. Other reagents were catalase (Boehringer-Mannheim GmbH, Mannheim, Germany), 2-[6-(4′-hydroxy)phenoxy-3H-xanthen-3-on-9-yl]benzoic acid (HPF, Daiichi, Tokyo, Japan), superoxide dismutase (SOD, Wako, Osaka, Japan), deferoxamine mesylate (Sigma), propidium iodide (PI, Sigma), chlormethiazole (CMZ, Sigma), diallyl sulphide (DAS, Tokyo Kasei Kogyo Co., Tokyo, Japan), diphenyl-1-pyrenylphosphine (DPPP, Dojindo, Kumamoto, Japan) and 3-(4,5-dimethylthiazol-2-yl)-2,5-diphenyltetrazolium bromide (MTT, Dojindo).

MTT assay

The MTT assay was used to test cell viability and cell growth as previously described [26]. In brief, HepG2 cells were seeded at 8×10^3 cells/well in 96 well plates and incubated at 37°C, 5% CO_2 for 24 h. MCLR at indicated concentrations was then added to each well. The cells were cultured for another 24, 48 or 72 h. Subsequently, 50 μL of 1 mg/ml MTT was added to each well followed by incubation at 37°C for 3 h. The medium was carefully aspirated and 100 μL DMSO was added to each well to dissolve the formed formazan crystals. Absorbance values at 570 nm were measured using a MPR-A4i microplate reader (Tosoh Corp., Tokyo, Japan). MTT reduction for each treatment was expressed as the percentage of the untreated control values.

LDH release assay

Lactate dehydrogenase (LDH) release from the cells was measured in 96 well plates using a CytoTox 96 non-radioactive cytotoxicity assay kit (Promega, Madison, WI). Briefly, HepG2 cells were treated with MCLR as described above. Contents in the wells were mixed with gentle pipetting, then the plate was centrifuged and the supernatants were taken for the LDH release assay. Formation of the formazan product at the end of the reaction was quantified. Total cellular LDH activity was measured in untreated cell lysates obtained by addition of 0.1% Triton X-100. LDH release into the medium was expressed as the percentage of total cellular LDH.

Cell cycle analysis

The proportions of the cells in G0/G1, S and G2/M phases were calculated from DNA content histograms obtained by flow cytometric analysis of cells stained with propidium iodide (PI). Briefly, HepG2 cells (8×10^4/well) were incubated in 12 well plates for 24 h. After treatment with MCLR for 24 or 48 h,

the cells were harvested using 0.25% Trypsin-EDTA, washed with PBS and then fixed with 70% ethanol at −20°C overnight. The fixed cells were stained with PI (50 μg/ml in PBS) at 37°C for 30 min in the presence of RNase (100 μg/ml). The stained cells were then analysed on BD FACScan (Becton Dickinson, San Jose, CA). At least 10 000 cells were collected for each sample, the percentage of cells in different phases of the cell cycle was determined using Cylchred software (Ver 1.0.2, CytonetUK, University of Wales College of Medicine, UK). Cells in sub-G1 fraction were considered as apoptotic cells.

Comet assay

HepG2 cells (1.6×10^5/dish) were plated in 35-mm dishes and incubated for 24 h. After incubation with MCLR for another 24 h, the cells were harvested by 0.25% Trypsin-EDTA and washed with PBS. The comet assay, that determines DNA strand breaks in individual cells, was performed as previously described by Li et al. [27]. One hundred cells from two slides were randomly selected to analyse tail moment using SCG image analysis software (DHS-SCG, version 1.0, KEIO Electronic Ind., Co., Ltd., Ibaraki, Japan). The tail moment was calculated as previously described [28]. For the individual cell, the DNA damage was graded according to the percentage of DNA in the tail (grade 0, no damage, < 5%; grade 1, low level damage, 5–20%; grade 2, medium level damage, 20–40%; grade 3, high level damage, 40–95%; grade 4, severe damage, > 95%) [29].

Immunostaining of 8OHdG

HepG2 cells were treated with MCLR for 24 h and 8OHdG staining was performed as previously described [30]. Briefly, the cells were fixed with cold 70% ethanol at −20°C for 10 min, treated with RNase (100 μg/ml) at 37°C for 1 h and proteinase K (10 μg/ml) for 5 min at room temperature, then the DNA was denatured with 4 N HCl for 7 min at room temperature. The cells were incubated with anti-8OHdG or its isotype control IgG1 (both 33.3 μg/ml) at 4°C overnight. The antibody-bound 8OHdG was visualized using Vectastain ABC and DAB Kits (Vector Laboratories, Burlingame, CA) according to the manufacturer's instructions. Five randomly selected fields were photographed on a microscope using a Pixera Penguin 150CL digital camera with Pixera Viewfinder 3.0 (Pixera Co., Los Gatos, CA). The staining intensity of 8OHdG in individual cell was quantified using Image-Pro Plus (version 4.0, Media Cybernetics, Silver Spring, MD).

Determination of lipid peroxide

Membrane lipid peroxides were detected using DPPP, a specific fluorescent probe for lipid peroxide. DPPP reacts with lipid peroxide stoichiometrically to generate a fluorescent product, DPPP oxide (DPPP = O) [31]. To detect lipid peroxides, HepG2 cells were incubated with 50 μM DPPP at 37°C for 15 min immediately after exposure to MCLR for 4 h, The images for the cell-associated fluorescence (DPPP = O) were acquired on a fluorescent microscopy with excitation and emission wavelength of 350 nm and 398 nm, respectively, using a Pixera Penguin 150CL digital camera with Pixera Viewfinder 3.0. The DPPP = O fluorescent intensity was quantified as described for 8OHdG immunostaining analysis.

Detection of ROS production

Intracellular ROS in HepG2 cells were detected using HPF as a fluorescence probe [32,33]. Briefly, HepG2 cells were seeded in 35-mm dishes and incubated for 24 h. After a further incubation for 4 h with MCLR in Hanks' balanced salt solution (HBSS) containing 10 mM Hepes (pH 7.3), the cells were incubated with 10 μM HPF at 37°C for 15 min. Bioimages of HPF were obtained using CSU-10 confocal laser scanning unit (Yokogawa Electric Co., Tokyo, Japan) coupled to IX90 inverted microscope (Olympus Optical Co., Tokyo, Japan) and C5810-01 colour chilled 3CCD camera (Hamamatsu Photonics, Hamamatsu, Japan). HPF was excited at 488 nm and the emissions were filtered using a 515 nm barrier filter. Mean fluorescence intensity for individual cell was determined using IPLab Spectrum software (version 3.0, Scanalystics Inc., Fairfax, VA).

Real-time PCR analysis of cytochrome P450 isoforms mRNA

The mRNA expression of cytochrome P450 isoforms CYP1A1, 1A2 and 2E1 was determined by real-time PCR. Briefly, total RNA was isolated from HepG2 cells by Trizol reagent (Invitrogen, Carlsbad, CA) according to the manufacturer's instructions. cDNA was synthesized by reverse transcription of total RNA using reverse transcriptase (Toyobo, Osaka, Japan) and oligo-dT (Sigma). The resulting cDNA was amplified at the following conditions: 50°C for 2 min, 95°C for 10 min, followed by 40 cycles of 15 s at 95°C and 1 min at 60°C, using the SYBR Green PCR Master Mix (Applied Biosystems, Foster City, CA). Real-time PCR was performed using an ABI Prism 7000 Sequence Detection System (Applied Biosystems, Foster City, CA). PCR primers were CYP1A1 (sense 5′-CTT GGA CCT CCT TGG AGC TG, antisense 5′-CGA AGG AAG AGT GTC GGA AG) [34]; CYP1A2 (sense 5′-CAA TCA GGT GGT GGT GTC AG, antisense 5′-GCT CCT GGA CTG TTT TCT GC) [34]; CYP2E1 (sense 5′-ACC CGA GAC ACC ATT TTC AG, antisense 5′-TCC AGC ACA CAC TCG TTT TC) [34]; GAPDH (sense 5′-TGG ACC TGA CCT GCC GTC TA, antisense 5′-CCC TGT TGC TGT AGC CAA ATT

C) [35]. For each sample, relative expression level of each cytochrome P450 isoform mRNA was calculated using cycle time (Ct) values, which were normalized against GAPDH. Relative quantification (Fold Change) between different samples was then determined according to the $2^{-\Delta\Delta Ct}$ method [36].

Statistical analysis

All experiments were performed in duplicate. Data are presented as mean ± SEM (standard error of the mean) from at least three independent experiments. Data on the comet assay and real-time PCR analyses were analysed using non-parametric Mann–Whitney U-test, while other statistical analyses were performed using one-way analyses of variance (ANOVA) followed by Dunnett's test; $p < 0.05$ was considered to be statistically significant.

Results

Effects of ROS scavengers on MCLR-induced cytotoxicity in HepG2 cells

First, we evaluated the effect of MCLR on cell viability and cell growth in HepG2 cells using the MTT assay. We found that MCLR at high (30 and 100 μM), but not low (1–10 μM) concentrations decreased cell viability and cell growth in time-dependent manners (Figure 1A). Although ROS scavenger, catalase, suppressed MCLR cytotoxicity at 24 h, the differences did not reach a statistically significant level (data not shown). At 48 h and 72 h, catalase and SOD significantly inhibited MCLR-induced cytotoxicity (Figure 1B).

Then, we evaluated the cytotoxicity of MCLR on HepG2 cells using the LDH release assay. MCLR did not increase significant LDH release in HepG2 cells at concentrations tested when incubated for 24 h. However, significant LDH releases were observed when the cells were incubated with MCLR at 30 μM and higher concentrations for 48 or 72 h (Figure 1C). Moreover, catalase significantly inhibited MCLR-induced LDH release. SOD by itself inhibited the formation of formazan product in LDH assay (data not shown), thus we compared its effect on MCLR-induced LDH release by adding SOD with MCLR simultaneously (co-incubation) or after incubation with MCLR (post-incubation). SOD did suppress the cytotoxicity of MCLR (Figure 1D).

Effects of ROS scavengers on MCLR-induced cell cycle arrest in HepG2 cells

To determine if the decreased cell viability and cell growth in MCLR-treated HepG2 cells is associated

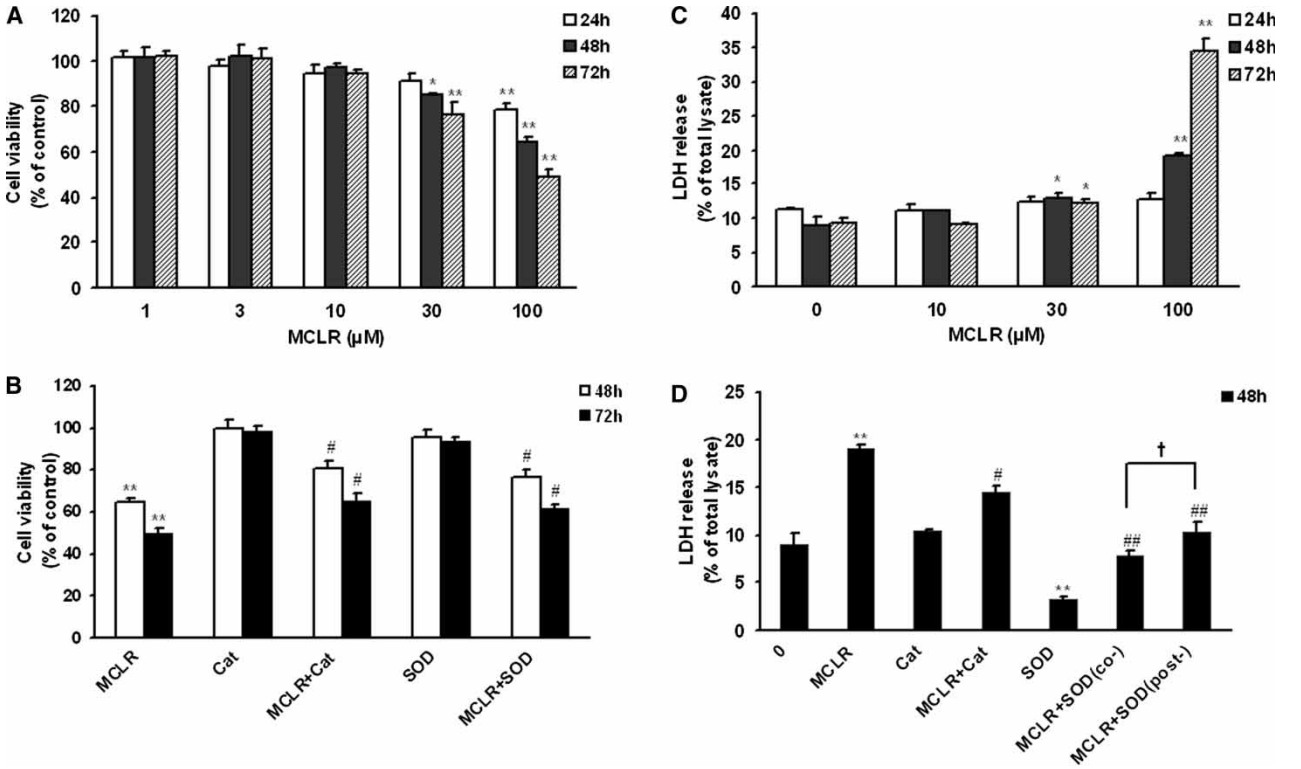

Figure 1. Effects of ROS scavengers on MCLR-induced cytotoxicity in HepG2 cells. (A) and (C) MCLR dose-dependently induced cytotoxicity determined by MTT and LDH release assays. (B) and (D) HepG2 cells were treated with 100 μM MCLR in the presence or absence of catalase (Cat, 1300 U/ml) or SOD (300 U/ml) at the indicated time periods. The data were presented as means ± SEM from three independent experiments conducted in duplicate. * $p < 0.05$ and ** $p < 0.01$ compared with untreated cells; # $p < 0.05$ and ## $p < 0.01$ compared with the cells treated with MCLR alone; † $p < 0.05$ significant difference between SOD added with MCLR simultaneously (co-, co-incubation) and SOD added after incubation with MCLR (post-, post-incubation) by Student's *t* test.

with changes in the cell cycle, we stained the cells with PI and analysed the proportions of the cells in different cell cycle phases. MCLR significantly increased the proportion of the cells in G0/G1 phase and correspondingly decreased the proportion of the cells in S phase in a time-dependent manner (Figure 2A). These effects could not be reversed by catalase, SOD or deferoxamine (data not shown). We found an increase in sub-G1 cell population after incubation with MCLR, indicating the increase in apoptosis. In contrast to the findings in cell cycle, three ROS scavengers significantly inhibited the effect of MCLR on sub-G1 cell population (Figure 2B).

Effects of ROS scavengers on MCLR-induced DNA damage in HepG2 cells

To evaluate whether MCLR causes DNA damage in HepG2 cells, we examined DNA strand breaks by the comet assay. MCLR at high (30 and 100 μM), but not low (1–10 μM) concentrations significantly increased DNA strand breaks as indicated by increased tail moments (Figure 3A and B). The percentage of the control cells with DNA strand breaks was $14.0 \pm 2.3\%$, whereas it increased to $63.9 \pm 3.5\%$ in cells treated with 100 μM MCLR. The majority of the cells that had DNA strand breaks were scored as Grade 1–2. Catalase, SOD and deferoxamine effectively suppressed MCLR-induced DNA strand break as shown by the decrease in tail moments (Figure 3C).

Next, we used quantitative immunostaining of 8OHdG to determine if MCLR increased oxidative DNA damage in HepG2 cells. As shown in Figure 4A, 8OHdG was localized mainly in the nucleus of both control and MCLR treated cells. MCLR increased 8OHdG in a dose-dependent manner. A significant increase in 8OHdG induction was observed at MCLR concentrations higher than 10 μM ($p < 0.01$). Similar to DNA strand breaks, catalase, SOD and deferoxamine significantly inhibited MCLR-induced 8OHdG formation (Figure 4B).

Effects of ROS scavengers on MCLR-induced lipid peroxidation in HepG2 cells

To examine whether MCLR causes oxidative lipid damage, we determined the formation of lipid peroxides in HepG2 cells using DPPP as a fluorescent probe. MCLR increased lipid damages significantly as indicated by the appearance of DPPP = O-derived fluorescence. The fluorescent staining was confined to the cell membrane, but not nucleus (Figure 5A). Catalase, SOD and deferoxamine almost completely inhibited DPPP = O-dependent fluorescence (Figure 5B).

Effects of MCLR on ROS generation in HepG2 cells

Using a laser confocal microscopy with HPF as a fluorescent probe, we examined whether MCLR induces the generation of ROS in HepG2 cells. HPF selectively detects intracellular hydroxyl radical ($^{\bullet}OH$), but not other ROS [33]. As shown in Figure 6A and B, a low level of ROS as indicated by the weak HPF fluorescence was observed in untreated cells. Exposure to 100 μM MCLR for 4 h significantly increased intracellular ROS level in HepG2 cells ($p < 0.001$).

Effects of MCLR on the mRNA expression of cytochrome P450 enzymes

To examine the potential sources of MCLR-induced ROS generation, we analysed the mRNA expression of ROS-generating enzymes cytochrome P450 isoforms including CYP1A1, 1A2 and 2E1 using real-time PCR analysis. The mRNA for CYP1A1 was constitutively expressed at a relatively high level in untreated cells. MCLR did not affect the expression of CYP1A1. In contrast, a low level of CYP2E1 mRNA expression was detected in untreated cells and it was significantly upregulated after exposure to 100 μM MCLR for 4 h (Figure 7). The expression

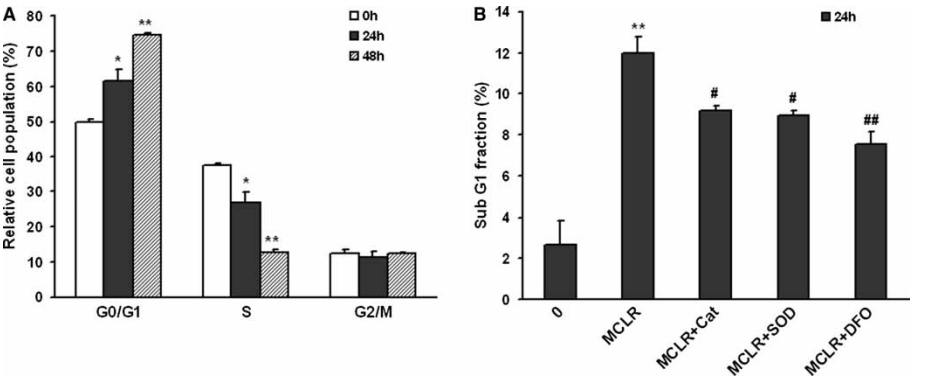

Figure 2. Effects of ROS scavengers on MCLR-induced cell cycle arrest in HepG2 cells. HepG2 cells were treated for 24 h or 48 h with 100 μM MCLR in the presence or absence of catalase (Cat, 1300 U/ml), SOD (300 U/ml) or deferoxamine (DFO, 1 mM) and stained with propidium iodide. (A) Cell cycle distribution was assessed by flow cytometry. (B) Apoptotic cells were estimated by determination of the cell proportion in sub-G1 fraction. The data were presented as means ± SEM from three independent experiments. * $p < 0.05$ and ** $p < 0.01$ compared with untreated cells; # $p < 0.05$ compared with the cells treated with MCLR alone.

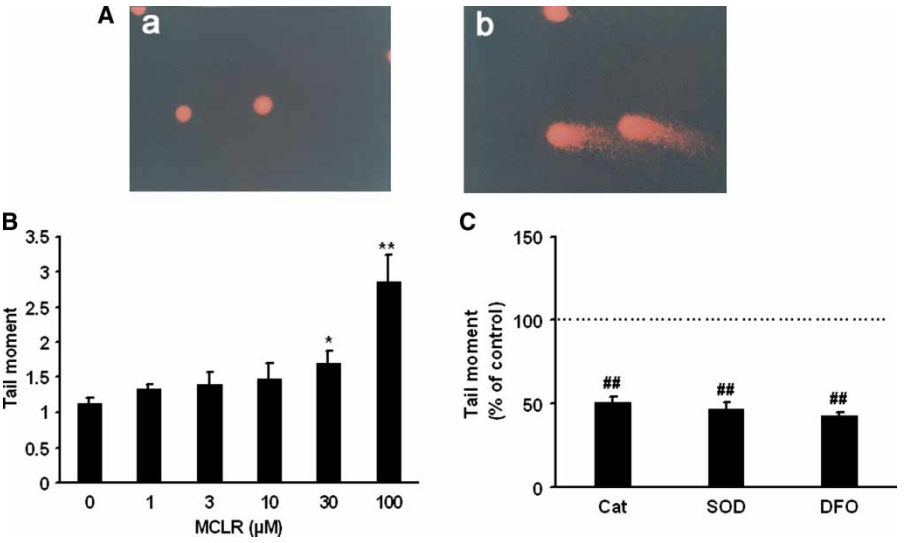

Figure 3. Effects of ROS scavengers on MCLR-induced DNA strand breaks expressed as tail moment in HepG2 cells. (A) These are the representative comet assay images showing DNA strand breaks in HepG2 cells treated with 100 μm MCLR (b) and medium alone (a) for 24 h. (B) MCLR dose-dependently induced DNA strand breaks as indicated by increased tail moment. (C) HepG2 cells were treated with 100 μm MCLR for 24 h in the presence or absence of catalase (Cat, 1300 U/ml), SOD (300 U/ml) or deferoxamine (DFO, 1 mm). DNA strand breaks in each scavenger-treated group are expressed as the percentage of that in cells treated with MCLR alone where the value is set as 100%. The data were presented as means ± SEM from three independent experiments conducted in duplicate. * $p < 0.05$ and ** $p < 0.01$ compared with untreated cells; ## $p < 0.01$ compared with the cells treated with MCLR alone.

level of CYP1A2 was extremely low in both control and MCLR-treated cells (data not shown).

Effects of CYP2E1 inhibitors on MCLR-induced ROS generation and cytotoxicity in HepG2 cells

To confirm the role of CYP2E1 in ROS generation by MCLR, we examined the effects of CYP2E1 inhibitors on MCLR-induced ROS generation in HepG2 cells. As shown in Figure 6B, in the presence of CYP2E1 inhibitors DAS and CMZ, the intracellular levels of ROS in MCLR-treated cells ($p < 0.01$) were similar to that in control (medium alone) cells. In addition, DAS and CMZ also significantly inhibited MCLR-induced cytotoxicity determined by the LDH release assay (Figure 8).

Discussion

Organic anion transporting polypeptides OATP1B1 and OATP1B3 are considered to be necessary for the hepatic uptake of MCLR [8–10]. MCLR induced potent cytotoxicity in OATP-transfected HEK293 and HeLa cells, as well as *xenopus* oocytes. These transfected cells have been reported to be more sensitive toward MCLR than primary rat hepatocytes [9,10]. The metabolic differences may be responsible for the differences in sensitivity toward MCLR between transfected non-hepatic cells and primary hepatocytes. MCLR is a potent hepatotoxin and the main target organ of MCLR is liver. Hepatocytes have a different metabolic system from other cell types. The human hepatoma cell line, HepG2, expresses a variety of xenobiotic metabolizing enzymes, particularly ROS-generating enzymes such as cytochrome P450 and NADPH oxidase, although the expression levels of some cytochrome P450 isoforms are lower than that of primary human hepatocytes [18–21]. Additionally, HepG2 cells express antioxidant enzymes such as SOD, catalase and glutathione peroxidase on a par with or more than that of primary human hepatocytes [21]. Therefore, HepG2 cells may be of great help to identify pro-oxidants and antioxidants of *in vivo* relevance [21]. Substantial evidence has shown that MCLR can be taken into HepG2 cells through non-specific transport mechanisms other than OATP, although they lack noteworthy OATP expression [22,37]. Zegura et al. [23] also demonstrated that exposure to MCLR (1 μM) did, in fact, have induced time-dependent alteration of intracellular reduced glutathione (GSH) levels in HepG2 cells. From these findings, we used HepG2 cells with metabolic system similar to human hepatocytes to investigate the role and possible mechanisms of ROS generation in MCLR-induced cytogenotoxicity.

We showed that MCLR at high concentrations (30 and 100 μM) suppressed cell viability and cell growth in HepG2 cells using the MTT assay (Figure 1A). It has been demonstrated that MCLR does not permeate the cell membrane and requires organic anion transporting polypeptides, OATP1B1 and OATP1B3 [8–10], for its uptake at low concentrations. Thus a higher concentration of MCLR might be required for its cytotoxicity in HepG2 cells. ROS scavengers, catalase and SOD, partially inhibited the suppression

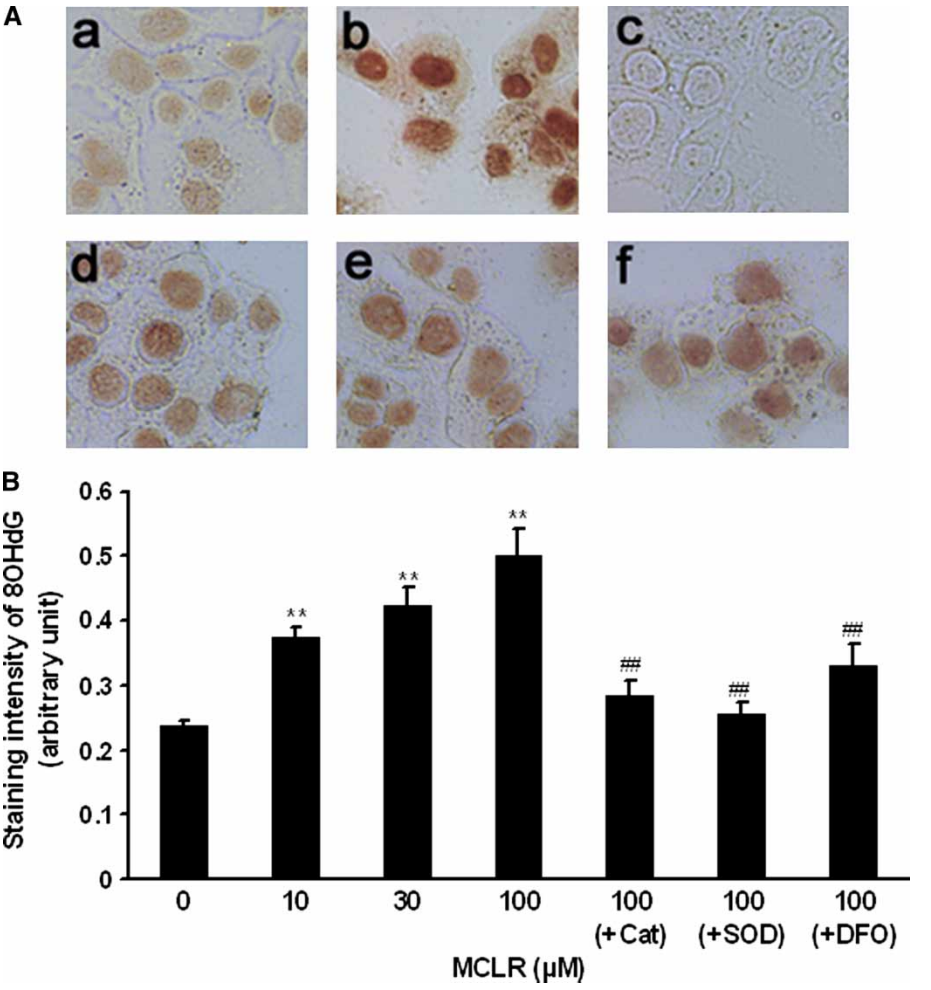

Figure 4. Effects of ROS scavengers on MCLR-induced 8OHdG in HepG2 cells. (A) These are the representative images for anti-8OHdG mAb immunostaining in HepG2 cells. (a) without MCLR; (b) incubated with 100 μm MCLR for 24 h; (c) control IgG1 staining in 100 μm MCLR-treated HepG2 cells; (d–f) incubated with 100 μm MCLR for 24 h in the presence of catalase (Cat, 1300 U/ml), SOD (300 U/ml) or deferoxamine (DFO, 1 mm), respectively. (B) Staining intensities of 8OHdG were analysed by Image-Pro Plus as described in the Materials and methods section. The data were presented as means ± SEM from three independent experiments. ** $p < 0.01$ compared with the untreated cells; ## $p < 0.01$ compared with the cells treated with MCLR alone.

in cell viability and cell growth induced by MCLR (Figure 1B). These findings indicate that ROS is in part involved in MCLR-induced cytotoxicity. Our results are consistent with previous reports [11,12]. Another ROS scavenger, deferoxamine (1 mM), was toxic to HepG2 cells when incubated for 48 h (data not shown). Therefore, we did not use deferoxamine in MTT and LDH release assays.

We then investigated whether MCLR induces DNA damage. The comet assay showed that MCLR at high (30 and 100 μM), but not low (1–10 μM) concentrations significantly increased DNA strand breaks in HepG2 cells after a 24-h exposure (Figure 3A and B). Catalase, SOD and deferoxamine significantly inhibited the formation of DNA strand breaks (Figure 3C). These findings indicate that ROS are involved in MCLR-induced DNA damage. Zegura et al. [24,25] previously reported that MCLR at non-toxic concentration (0.01–1 μM) increased DNA strand breaks in HepG2 cells. However, the damage they observed was transient or reversible because it declined with further exposure to toxin. DNA strand breaks can be caused by multiple factors including ROS and thus are not specific for oxidative DNA damage [38,39]. By analysing 8OHdG, which is a specific oxidative DNA damage product [40–43], we found that MCLR even at non-cytotoxic concentrations significantly increased the levels of 8OHdG, suggesting that the observed DNA damage is not the consequence of the cytotoxicity. Consistent with our findings, a previous report showed that MCLR increased 8OHdG in primary rat hepatocytes [44]. The suppressive effects of catalase, SOD and deferoxamine on 8OHdG induction further confirm that ROS are generated in this system.

The results of LDH release assay showed that MCLR caused membrane damage and cell death in HepG2 cells when incubated for 48 h (Figure 1C), and that MCLR-induced membrane damage and

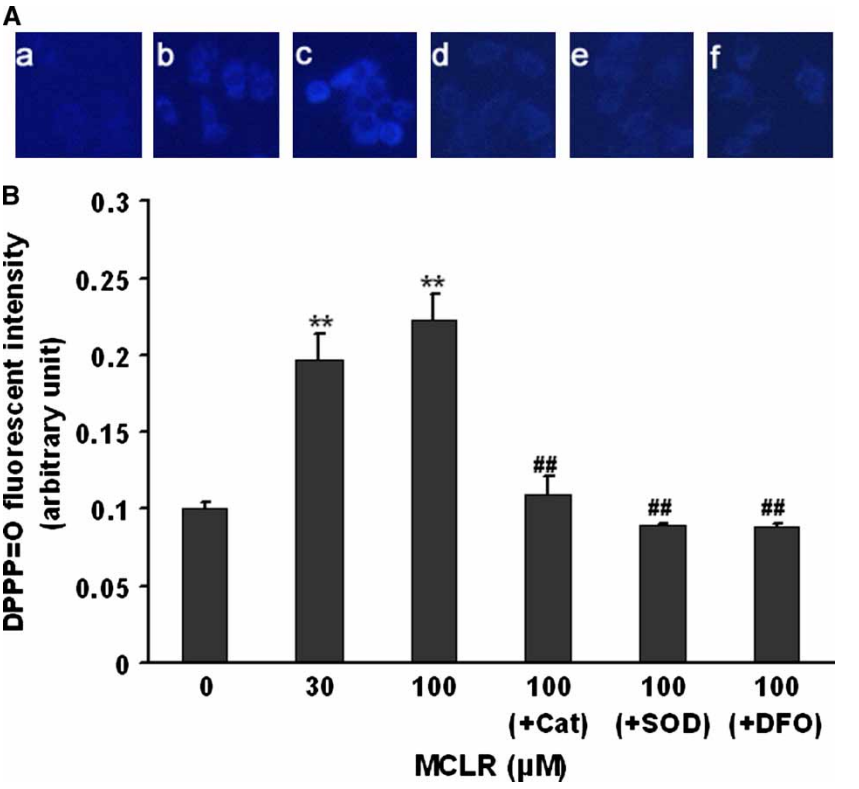

Figure 5. Effects of ROS scavengers on MCLR-induced lipid peroxidation in HepG2 cells. (A) These are the representative fluorescent images showing the presence of lipid peroxides, as determined by fluorescent probe DPPP, on the membrane of HepG2 cells. (a) without MCLR; (b) or (c) incubated with 30 or 100 μM MCLR for 4 h; (d–f) incubated with 100 μM MCLR for 4 h in the presence of catalase (Cat, 1300 U/ml), SOD (300 U/ml) or deferoxamine (DFO, 1 mM), respectively. (B) DPPP oxides-dependent fluorescence intensities were analysed by Image-Pro Plus as described in the Materials and methods section. The data were presented as means ± SEM from three independent experiments. ** $p < 0.01$ compared with the untreated cells; ## $p < 0.01$ compared with the cells treated with MCLR alone.

cell death could be reversed by catalase and SOD (Figure 1D). In support for this, Ding et al. [12] reported that MCLR induced-ROS generation preceded the MCLR-induced LDH release in rat hepatocytes. Membrane lipid peroxidation is a ROS-mediated specific membrane damage. Using DPPP as a specific lipid peroxide probe, we directly demonstrated the formation of lipid peroxides on the membrane of MCLR-treated cells as shown by the increased DPPP = O-dependent fluorescence (Figure 5A). The complete abortion of DPPP = O-dependent fluorescence by catalase, SOD and deferoxamine

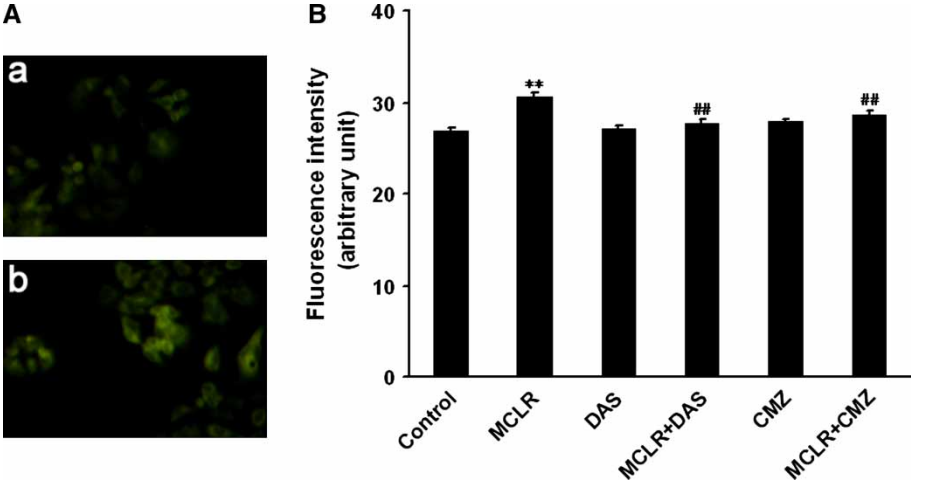

Figure 6. Effects of MCLR on intracellular ROS generation in HepG2 cells. (A) These are the representative fluorescent images showing the presence of intracellular ROS in HepG2 cells treated with 100 μm MCLR (b) and medium alone (a) for 4 h. (B) HepG2 cells were treated with 100 μm MCLR for 4 h in the presence or absence of DAS (2 mm) or CMZ (20 μm, pre-treated for 6 h). HPF fluorescence intensities were quantified using IPLab Spectrum software. The data were presented as means ± SEM from three independent experiments. ** $p < 0.01$ compared with the untreated cells; ## $p < 0.01$ compared with the cells treated with MCLR alone.

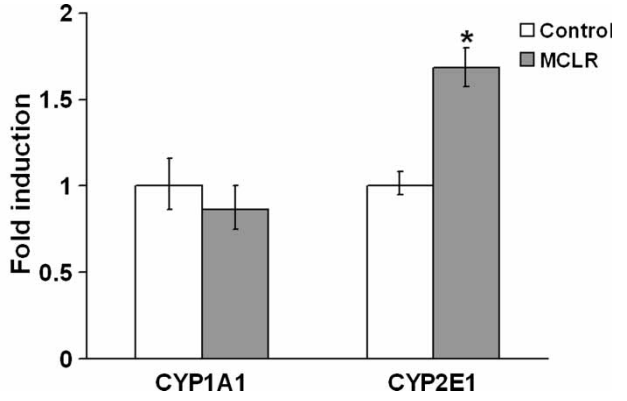

Figure 7. Effect of MCLR on the expression of CYP1A1 and CYP2E1 mRNA in HepG2 cells. HepG2 cells were treated with or without 100 μM MCLR for 4 h, then total RNA was extracted and the mRNA expression of cytochrome P450 isoforms CYP1A1 and 2E1 were analysed by real-time PCR as described in the Materials and methods section. The data were presented as mean value with the range (minimum and maximum) from four independent experiments conducted in triplicate. * $p < 0.05$ compared with the untreated cells.

(Figure 5B) further supports that lipid peroxidation on MCLR-treated cell membrane is caused by ROS.

The induction of oxidative DNA and lipid damages by MCLR in HepG2 cells encourage us to directly examine whether ROS are generated in MCLR-treated cells using HPF, a new fluorescence probe. Unlike dichlorofluorescin diacetate (DCFH-DA), HPF, which is resistant to light-induced autooxidation, selectively and dose-dependently generates a strong fluorescent compound, fluorescein, upon reaction with •OH, but not other ROS [32,33,45]. These advantages thus allow us to quantitatively analyse ROS in cells more correctly. We demonstrated that MCLR increased intracellular ROS levels in HepG2 cells (Figure 6A and B). Further, using

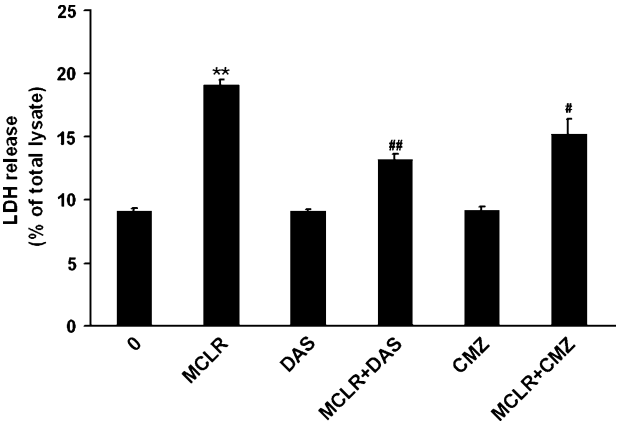

Figure 8. Effects of CYP2E1 inhibitors on MCLR-induced cytotoxicity in HepG2 cells. HepG2 cells were treated with 100 μM MCLR for 48 h in the presence or absence of DAS (2 mM) or CMZ (20 μM, pre-treated for 6 h) and then subjected to the LDH release assay. The data were presented as means ± SEM from three independent experiments conducted in duplicate. ** $p < 0.01$ compared with untreated cells; # $p < 0.05$ and ## $p < 0.01$ compared with the cells treated with MCLR alone.

DMPO as an ESR spin trapper we also detected the presence of •OH in MCLR-treated cells. Catalase, SOD and deferoxamine decreased the intensity of the DMPO-OH signals (data not shown). These findings indicate that MCLR increased the generation of ROS and the detected, •OH was derived from the Fenton reaction.

We further analysed the mechanisms by which MCLR produces ROS. Several studies have identified NADPH oxidase and cytochrome P450 as potential sources for the generation of ROS in HepG2 cells [46–50]. Thus, to clarify the major site of ROS generation in MCLR-treated cells we investigated whether MCLR affects the phosphorylation of NADPH oxidase and the expression of cytochrome P450. Because it is so hard to obtain enough amounts of MCLR from chemical company that 100 μM MCLR-treated cells were extremely limited, we were unable to demonstrate if $p47^{phox}$, one of the components of NADPH oxidase [48], is related to ROS generation by MCLR using Western blot analysis. It has been shown that the over-expression of cytochrome P450 isoforms CYP1A1, 1A2 and 2E1 increased ROS generation in lymphocytes and HepG2 cells [50,51]. We showed here that MCLR significantly upregulated the expression of CYP2E1 mRNA, but not CYP1A1 mRNA (Figure 7). The expression level of CYP1A2 was extremely low in both control and MCLR-treated cells, thus we could not analyse its expression. As reported by Gonzalez [50], CYP2E1 mRNA was constitutively expressed at a low level in untreated HepG2 cells. However, its expression could be detected using real-time PCR analysis. CYP2E1 exhibits NADPH oxidase activity and is the most active form of ROS-generating cytochrome P450. It generates ROS such as $O_2^{\bullet -}$ and H_2O_2 during its catalytic cycle even in the absence of substrate. It also produces powerful oxidants such as •OH in the presence of iron catalysts [50,52]. Therefore, the upregulation of CYP2E1 observed in our study might contribute to MCLR-induced •OH generation in the presence of iron. CMZ has been reported to specifically inhibit the induction of CYP2E1 at the mRNA and protein levels [53], while DAS inactivates CYP2E1 activity via a suicide-inhibitory action [54]. Both CMZ and DAS decreased the elevated intracellular level of ROS (Figure 6B). CMZ and DAS also inhibited MCLR-induced LDH release (Figure 8), suggesting the involvement of CYP2E1 in MCLR-induced cytogenotoxicity in HepG2 cells. CYP2E1 might be a potential source of ROS generation by MCLR.

Although ROS scavengers prevented DNA damage, lipid damage and extracellular LDH release caused by MCLR, they had weak inhibitory effects on total cytotoxicity of MCLR as measured by the MTT assay. These findings suggest additional mechanism(s) other than ROS in MCLR-induced

cytotoxicity. Because the MTT assay detects both cell viability and cell growth [55], we then analysed the effects of MCLR on cell cycle. We found that MCLR decreased the cells in S phase and increased the cells in G1 phase, indicating that MCLR induced cell cycle arrest. Further, the ROS scavengers did not reverse the cell cycle arrest. The cell cycle is controlled by the phosphorylation of cyclin-dependent kinase inhibitors (CKIs), cyclin-dependent kinases (CDKs) and other regulatory proteins of CDK [56,57]. It has been reported that MCLR potently inhibited PP1 and PP2A [5–7]. Thus, we speculate that MCLR may change the phosphorylation of these regulatory proteins and thus causes cell cycle arrest. We found that MCLR increased sub-G1 cell population, indicating an increase in apoptotic cells and that ROS scavengers were able to reverse the effect of MCLR on sub-G1 cell population. This helps explain why ROS scavengers showed less effects on cytotoxicity of MCLR as measured by the MTT assay.

Addition of catalase, SOD or deferoxamine suppressed the cytogenotoxicity of MCLR in HepG2 cells. The inhibitory effect of deferoxamine is likely due to its chelation of iron in cells, while catalase probably exerts its effects by removing both intracellular and extracellular H_2O_2, because hydrogen peroxide can permeate the cell membrane freely [58]. On the other hand, some studies have observed rapid endocytosis of exogenously added SOD into rat hepatocytes and human endothelial cells [59–61]. Thus, the suppressive effect of SOD we observed in this study may be related to intracellular uptake of SOD via endocytosis.

In conclusion, MCLR caused the generation of ROS, subsequent induction of oxidative damages in lipid and DNA, which were suppressed by ROS scavengers, and upregulated the expression of CYP2E1 mRNA in HepG2 cells. MCLR also induced cell death partially due to the generation of ROS. In addition, CYP2E1 inhibitors suppressed MCLR-induced ROS generation and cytotoxicity. Thus, CYP2E1 might be a potential source of ROS generation by MCLR. Further studies are required to clarify the mechanisms of induction of CYP2E1 by MCLR and the relationship between oxidative stress and perturbation in protein phosphorylation induced by MCLR.

Acknowledgements

This work was supported by grants from Grants-in-Aid for Scientific Research awarded by the Ministry of Education, Science, Sports and Culture of Japan (#14370140 and #18390183). The authors express thanks to Miss Miharu Ushikai (Graduate School of Medical and Dental Sciences, Kagoshima University) for her excellent technical assistance.

References

[1] Carmichael WW. Cyanobacteria secondary metabolites: the cyanotoxins. J Appl Bacteriol 1992;72:445–459.
[2] Carmichael WW. The toxins of cyanobacteria. Sci Am 1994;270:78–86.
[3] Ho L, Onstad G, von Gunten U, Rinck-Pfeiffer S, Craig K, Newcombe G. Differences in the chlorine reactivity of four microcystin analogues. Water Res 2006;40:1200–1209.
[4] Sekijima M, Tsutsumi T, Yoshida T, Harada T, Tashiro F, Chen G, Yu SZ, Ueno Y. Enhancement of glutathione S-transferase placental-form positive liver cell foci development by microcystin-LR in aflatoxin B1-initiated rats. Carcinogenesis 1999;20:161–165.
[5] Honkanen RE, Zwiller J, Moore RE, Daily SL, Khatra BS, Dukelow M, Boynton AL. Characterization of microcystin-LR, a potent inhibitor of type 1 and type 2A protein phosphatases. J Biol Chem 1990;265:19401–19404.
[6] MacKintosh C, Beattie KA, Klumpp S, Cohen P, Codd GA. Cyanobacterial microcystin-LR is a potent and specific inhibitor of protein phosphoatase 1 and 2A from both mammals and higher plants. FEBS Lett 1990;264:187–192.
[7] Gehringer MM. Microcystin-LR and okadaic acid-induced cellular effects: a dualistic response. FEBS Lett 2004;557:1–8.
[8] Fischer WJ, Altheimer S, Cattori V, Meier PJ, Dietrich DR, Hagenbuch B. Organic anion transporting polypeptides expressed in liver and brain mediate uptake of microcystin. Toxicol Appl Pharmacol 2005;203:257–263.
[9] Monks NR, Liu S, Xu Y, Yu H, Bendelow AS, Moscow JA. Potent cytotoxicity of the phosphatase inhibitor microcystin LR and microcystin analogues in OATP1B1- and OATP1B3-expressing HeLa cells. Mol Cancer Ther 2007;6:587–598.
[10] Komatsu M, Furukawa T, Ikeda R, Takumi S, Nong Q, Aoyama K, Akiyama S, Keppler D, Takeuchi T. Involvement of mitogen-activated protein kinase signaling pathways in microcystin-LR-induced apoptosis after its selective uptake mediated by OATP1B1 and OATP1B3. Toxicol Sci 2007;97:407–416.
[11] Ding WX, Shen HM, Ong CN. Critical role of reactive oxygen species and mitochondrial permeability transition in microcystin-induced rapid apoptosis in rat hepatocytes. Hepatology 2000;32:547–555.
[12] Ding WX, Shen HM, Ong CN. Critical role of reactive oxygen species formation in microcystin-induced cytoskeleton disruption in primary cultured hepatocytes. J Toxicol Environ Health A 2001;64:507–519.
[13] Ding WX, Shen HM, Ong CN. Calpain activation after mitochondrial permeability transition in microcystin-induced cell death in rat hepatocytes. Biochem Biophys Res Commun 2002;291:321–331.
[14] Ding WX, Nam Ong C. Role of oxidative stress and mitochondrial changes in cyanobacteria-induced apoptosis and hepatotoxicity. FEMS Microbiol Lett 2003;220:1–7.
[15] Botha N, Gehringer MM, Downing TG, van de Venter M, Shephard EG. The role of microcystin-LR in the induction of apoptosis and oxidative stress in CaCo2 cells. Toxicon 2004;43:85–92.
[16] Chen T, Wang Q, Cui J, Yang W, Shi Q, Hua Z, Ji J, Shen P. Induction of apoptosis in mouse liver by microcystin-LR: a combined transcriptomic, proteomic, and simulation strategy. Mol Cell Proteom 2005;4:958–974.
[17] Weng D, Lu Y, Wei Y, Liu Y, Shen P. The role of ROS in microcystin-LR-induced hepatocyte apoptosis and liver injury in mice. Toxicology 2007;232:15–23.

[18] Doostdar H, Demoz A, Burke MD, Melvin WT, Grant MH. Variation in drug-metabolising enzyme activities during the growth of human HepG2 hepatoma cells. Xenobiotica 1990;20:435–441.

[19] Knasmuller S, Parzefall W, Sanyal R, Ecker S, Schwab C, Uhl M, Mersch-Sundermann V, Williamson G, Hietsch G, Langer T, Darroudi F, Natarajan AT. Use of metabolically competent human hepatoma cells for the detection of mutagens and antimutagens. Mutat Res 1998;402:185–202.

[20] Knasmuller S, Mersch-Sundermann V, Kevekordes S, Darroudi F, Huber WW, Hoelzl C, Bichler J, Majer BJ. Use of human-derived liver cell lines for the detection of environmental and dietary genotoxicants; current state of knowledge. Toxicology 2004;198:315–328.

[21] Mersch-Sundermann V, Knasmuller S, Wu XJ, Darroudi F, Kassie F. Use of a human-derived liver cell line for the detection of cytoprotective, antigenotoxic and cogenotoxic agents. Toxicology 2004;198:329–340.

[22] Eriksson JE, Gronberg L, Nygard S, Slotte JP, Meriluoto JA. Hepatocellular uptake of ^{3}H-dihydromicrocystin-LR, a cyclic peptide toxin. Biochim Biophys Acta 1990;1025:60–66.

[23] Zegura B, Lah TT, Filipic M. Alteration of intracellular GSH levels and its role in microcystin-LR-induced DNA damage in human hepatoma HepG2 cells. Mutat Res 2006;611:25–33.

[24] Zegura B, Sedmak B, Filipic M. Microcystin-LR induces oxidative DNA damage in human hepatoma cell line HepG2. Toxicon 2003;41:41–48.

[25] Zegura B, Lah TT, Filipic M. The role of reactive oxygen species in microcystin-LR-induced DNA damage. Toxicology 2004;200:59–68.

[26] Komatsu M, Sumizawa T, Mutoh M, Chen ZS, Terada K, Furukawa T, Yang XL, Gao H, Miura N, Sugiyama T, Akiyama S. Copper-transporting P-type adenosine triphosphatase (ATP7B) is associated with cisplatin resistance. Cancer Res 2000;60:1312–1316.

[27] Li D, Morimoto K, Takeshita T, Lu Y. Formamidopyrimidine-DNA glycosylase enhances arsenic-induced DNA strand breaks in PHA-stimulated and unstimulated human lymphocytes. Environ Health Perspect 2001;109:523–526.

[28] Olive PL, Banath JP, Durand RE. Heterogeneity in radiation-induced DNA damage and repair in tumor and normal cells measured using the 'comet' assay. Radiat Res 1990;122:86–94.

[29] Ding WX, Shen HM, Zhu HG, Lee BL, Ong CN. Genotoxicity of microcystic cyanobacteria extract of a water source in China. Mutat Res 1999;442:69–77.

[30] Arima Y, Nishigori C, Takeuchi T, Oka S, Morimoto K, Utani A, Miyachi Y. 4-Nitroquinoline 1-oxide forms 8-hydroxydeoxyguanosine in human fibroblasts through reactive oxygen species. Toxicol Sci 2006;91:382–392.

[31] Takahashi M, Shibata M, Niki E. Estimation of lipid peroxidation of live cells using a fluorescent probe, diphenyl-1-pyrenylphosphine. Free Radic Biol Med 2001;31:164–174.

[32] Indo HP, Davidson M, Yen HC, Suenaga S, Tomita K, Nishii T, Higuchi M, Koga Y, Ozawa T, Majima HJ. Evidence of ROS generation by mitochondria in cells with impaired electron transport chain and mitochondrial DNA damage. Mitochondrion 2007;7:106–118.

[33] Setsukinai K, Urano Y, Kakinuma K, Majima HJ, Nagano T. Development of novel fluorescence probes that can reliably detect reactive oxygen species and distinguish specific species. J Biol Chem 2003;278:3170–3175.

[34] Shervington A, Mohammed K, Patel R, Lea R. Identification of a novel co-transcription of P450/1A1 with telomerase in A549. Gene 2007;388:110–116.

[35] Zhang X, Ding L, Sandford AJ. Selection of reference genes for gene expression studies in human neutrophils by real-time PCR. BMC Mol Biol 2005;6:4.

[36] Livak KJ, Schmittgen TD. Analysis of relative gene expression data using real-time quantitative PCR and the 2(-Delta Delta C(T)) method. Methods 2001;25:402–408.

[37] Abe T, Unno M, Onogawa T, Tokui T, Kondo TN, Nakagomi R, Adachi H, Fujiwara K, Okabe M, Suzuki T, Nunoki K, Sato E, Kakyo M, Nishio T, Sugita J, Asano N, Tanemoto M, Seki M, Date F, Ono K, Kondo Y, Shiiba K, Suzuki M, Ohtani H, Shimosegawa T, Iinuma K, Nagura H, Ito S, Matsuno S. LST-2, a human liver-specific organic anion transporter, determines methotrexate sensitivity in gastrointestinal cancers. Gastroenterology 2001;120:1689–1699.

[38] Halliwell B, Aruoma OI. DNA damage by oxygen-derived species. FEBS Lett 1991;281:9–19.

[39] Takeuchi T, Morimoto K. Crocidolite asbestos increased 8-hydroxydeoxyguanosine levels in cellular DNA of a human promyelocytic leukemia cell line, HL60. Carcinogenesis 1994;15:635–639.

[40] Kasai H, Nishimura S. Hydroxylation of deoxyguanosine at the C-8 position by ascorbic acid and other reducing agents. Nucleic Acids Res 1984;12:2137–2145.

[41] Takeuchi T, Nakajima M, Morimoto K. Establishment of a human system that generates O_2 and induces 8-hydroxydeoxyguanosine, typical of oxidative DNA damage, by a tumor promoter. Cancer Res 1994;54:5837–5840.

[42] Takeuchi T, Nakajima M, Morimoto K. Relationship between the intracellular reactive oxygen species and the induction of oxidative DNA damage in human neutrophil-like cells. Carcinogenesis 1996;17:1543–1548.

[43] Dizdaroglu M. Chemical determination of free radical-induced damage to DNA. Free Radic Biol Med 1991;10:225–242.

[44] Maatouk I, Bouaicha N, Plessis MJ, Perin F. Detection by ^{32}P-postlabelling of 8-oxo-7,8-dihydro-2′-deoxyguanosine in DNA as biomarker of microcystin-LR- and nodularin-induced DNA damage in vitro in primary cultured rat hepatocytes and in vivo in rat liver. Mutat Res 2004;564:9–20.

[45] Afzal M, Matsugo S, Sasai M, Xu B, Aoyama K, Takeuchi T. Method to overcome photoreaction, a serious drawback to the use of dichlorofluorescin in evaluation of reactive oxygen species. Biochem Biophys Res Commun 2003;304:619–624.

[46] Lee YS, Kang YS, Lee JS, Nicolova S, Kim JA. Involvement of NADPH oxidase-mediated generation of reactive oxygen species in the apototic cell death by capsaicin in HepG2 human hepatoma cells. Free Radic Res 2004;38:405–412.

[47] Kim JA, Lee YS. Role of reactive oxygen species generated by NADPH oxidase in the mechanism of activation of K(+)-Cl(−)-cotransport by N-ethylmaleimide in HepG2 human hepatoma cells. Free Radic Res 2001;35:43–53.

[48] Lee YS, Kang YS, Lee SH, Kim JA. Role of NAD(P)H oxidase in the tamoxifen-induced generation of reactive oxygen species and apoptosis in HepG2 human hepatoblastoma cells. Cell Death Differ 2000;7:925–932.

[49] Nieto N, Friedman SL, Cederbaum AI. Stimulation and proliferation of primary rat hepatic stellate cells by cytochrome P450 2E1-derived reactive oxygen species. Hepatology 2002;35:62–73.

[50] Gonzalez FJ. Role of cytochromes P450 in chemical toxicity and oxidative stress: studies with CYP2E1. Mutat Res 2005;569:101–110.

[51] Puntarulo S, Cederbaum AI. Production of reactive oxygen species by microsomes enriched in specific human cytochrome P450 enzymes. Free Radic Biol Med 1998;24:1324–1330.

[52] Dey A, Cederbaum AI. Geldanamycin, an inhibitor of Hsp90 increases cytochrome P450 2E1 mediated toxicity in HepG2 cells through sustained activation of the p38MAPK pathway. Arch Biochem Biophys 2007;461:275–286.

[53] Tindberg N, Baldwin HA, Cross AJ, Ingelman-Sundberg M. Induction of cytochrome P450 2E1 expression in rat and gerbil astrocytes by inflammatory factors and ischemic injury. Mol Pharmacol 1996;50:1065–1072.

[54] Brady JF, Ishizaki H, Fukuto JM, Lin MC, Fadel A, Gapac JM, Yang CS. Inhibition of cytochrome P-450 2E1 by diallyl sulfide and its metabolites. Chem Res Toxicol 1991;4:642–647.

[55] Mosmann T. Rapid colorimetric assay for cellular growth and survival: application to proliferation and cytotoxicity assays. J Immunol Methods 1983;65:55–63.

[56] Dynlacht BD. Regulation of transcription by proteins that control the cell cycle. Nature 1997;389:149–152.

[57] Lew DJ, Kornbluth S. Regulatory roles of cyclin dependent kinase phosphorylation in cell cycle control. Curr Opin Cell Biol 1996;8:795–804.

[58] Halliwell B, Whiteman M. Measuring reactive species and oxidative damage in vivo and in cell culture: how should you do it and what do the results mean? Br J Pharmacol 2004;142:231–255.

[59] Kyle ME, Nakae D, Sakaida I, Miccadei S, Farber JL. Endocytosis of superoxide dismutase is required in order for the enzyme to protect hepatocytes from the cytotoxicity of hydrogen peroxide. J Biol Chem 1988;263:3784–3789.

[60] Li L, Wattiaux-De Coninck S, Wattiaux R. Endocytosis of superoxide dismutase by rat liver. Biochem Biophys Res Commun 1992;184:727–732.

[61] Waelti ER, Barton M. Rapid endocytosis of copper-zinc superoxide dismutase into human endothelial cells: role for its vascular activity. Pharmacology 2006;78:198–201.